

Single hole dynamics in the t - J model on two- and three-leg ladders

Michael Brunner^{1,2}, Sylvain Capponi^{1,3}, Fakhre F. Assaad¹, and Alejandro Muramatsu¹

¹*Institut für Theoretische Physik III, Universität Stuttgart, Pfaffenwaldring 57, D-70550 Stuttgart, Germany*

²*School of Physics, The University of New South Wales, Sydney, NSW 2052, Australia*

³*Université Paul Sabatier, Laboratoire de Physique Quantique, 118 route de Narbonne, 31062 Toulouse, France*
(October 30, 2018)

The dynamics of a single hole in the t - J model on two- (2LL) and three- (3LL) leg ladders is studied using a recently developed quantum Monte Carlo algorithm. For the 2LL it is shown that in addition to the most pronounced features of the spectral function, well described by the limit of strong coupling along the rungs, a clear shadow band appears in the antibonding channel. Moreover, both the bonding band and its shadow have a finite quasiparticle (QP) weight in the thermodynamic limit. For strong coupling along the rungs of the 3LL, the low-energy spectrum in the antisymmetric channel is similar to a one-dimensional chain, whereas in the two symmetric channels it resembles the 2LL. The QP weight vanishes in the antisymmetric channel, but is finite in the symmetric one.

The n -leg ladder systems serve as a bridge from one-dimensional chains to two-dimensional layered cuprates, offering thus a rich playground for studying the interplay of charge and spin degrees of freedom in strongly correlated systems^{1,2}. In particular, two- (2LL) and three- (3LL) leg ladder materials became recently available, making experiments possible in such systems³. At zero doping, the spin-excitation spectrum is gapped in the case of even-leg ladders, whereas it is gapless in the case of an odd number of legs, as found by experiments on 2LL and 3LL^{2,3} and by quantum Monte Carlo (QMC) simulations of up to five-leg ladders⁴. A discussion on the impact of this odd-even effect on the charge excitation spectrum as obtained by angle resolved photoemission (ARPES) experiments has recently started⁵.

Charge carriers on cuprates can be well described by the t - J model⁶. For the 2LL a considerable amount of work has been done by exact diagonalizations (ED)⁷⁻⁹, density-matrix renormalization group (DMRG)¹⁰, and strong coupling expansions^{11,12}, leading to the following picture: When the coupling along the rungs J_{\perp} is much larger than along the chains (J_{\parallel}), the bonding and the antibonding band are split by $2t_{\perp}$. The bonding band shows a sharp peak at the lower edge of the spectrum. Approaching the isotropic case, the energy gap between the bonding and antibonding band is reduced, and the bands become nearly flat on half of the Brillouin zone. Results of exact diagonalizations⁸ indicate, that spin and charge excitations are coupled to each other, leading to the existence of quasiparticles in these systems. Like for the 2LL, the strong-coupling limit of the 3LL is a promising starting point. In this limit, the low-energy excitations have odd parity, and can be described by an effective one-dimensional (1D) t - J -model¹³, which forms a Luttinger liquid in a wide parameter range of J/t . Results from ED of three-leg ladders suggest that the two even channels have the same physics as 2LL⁵ up to the isotropic case. However, due to the small systems considered, the gap between the even and the odd channel

is of the same order as the finite-size spin-gap. Whether a particular channel will evolve upon doping towards the Luttinger-Tomonaga or the Luther-Emery universality class is signaled by the absence or not of a quasiparticle (QP) weight in the single hole case. This can only be determined by performing a finite-size scaling. Whereas a Mott-insulator with branch cuts in the spectral function (i.e. without QP) evolves towards a Luttinger-liquid upon doping, the Luttinger-liquid parameter reaches the universal value $K_{\rho} = 1$ in the limit of zero doping for a spin-gapped system¹⁴. Then, using a previous analysis of the spectral function for Luther-Emery systems¹⁵ a finite QP weight in the single hole case results.

In this paper we study single hole dynamics in the t - J model on 2LL and 3LL using a recently developed QMC algorithm, which has been successfully applied to one¹⁶ and two dimensions¹⁷. The spin dynamics is efficiently simulated by a loop-algorithm¹⁸ and for each spin configuration, the one-particle Green's function is calculated exactly. For details see Ref. 17. The QP weight and dispersion are determined from the asymptotics in imaginary time of the Green's function and the full spectral function is obtained with the Maximum Entropy method¹⁹.

The t - J model is given by

$$H = - \sum_{\langle i,j \rangle} t_{ij} \tilde{c}_{i,\sigma}^{\dagger} \tilde{c}_{j,\sigma} + \sum_{\langle i,j \rangle} J_{ij} (\vec{S}_i \cdot \vec{S}_j - \frac{1}{4} \tilde{n}_i \tilde{n}_j), \quad (1)$$

where \tilde{c}_i^{\dagger} are electron operators restricted to the Hilbert space with no double occupancy, $\vec{S}_i = (1/2) \sum_{\alpha,\beta} c_{i,\alpha}^{\dagger} \vec{\sigma}_{\alpha,\beta} c_{i,\beta}$, $\tilde{n}_i = \sum_i \tilde{c}_i^{\dagger} \tilde{c}_i$ and the sum $\langle i,j \rangle$ runs over nearest neighbors only. For i,j on a rung we set $J_{ij} = J_{\perp}$, $t_{ij} = t_{\perp}$, and $J_{ij} = J_{\parallel}$, $t_{ij} = t_{\parallel}$ if i,j are on the same leg ($t \equiv t_{\parallel}$ is the unit of energy in the following). Along the legs of the ladder we use periodic boundary conditions, whereas the boundaries are open along the rungs. The reference energy is the Heisenberg groundstate.

We start our discussion with the 2LL in the limit $J_{\perp} \gg J_{\parallel}$. At half filling, this leads to the formation of singlets on each rung²⁰. Perturbative treatments¹¹ or series expansions¹² around this limit show that, like in the free case, the hole has a cosine-like dispersion with a splitting of the bonding and the antibonding bands by t_{\perp} . The only difference is a rescaling of the effective hopping to $-t_{\parallel}/2$ and a shift of the energies by J_{\perp} .

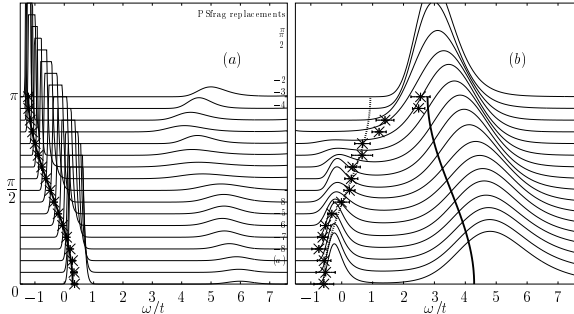


FIG. 1. Quasiparticle dispersion and spectral function for the bonding (a) and the antibonding (b) band for the 2LL with $J_{\perp}/t_{\parallel} = 1.6$, $J_{\parallel}/t_{\parallel} = 0.4$, and $t_{\perp}/t_{\parallel} = 2$. Further details are discussed in the text.

Figure 1 presents our results for a 2LL with 2×32 sites, where $J_{\parallel}/t_{\parallel} = 0.4$, $J_{\perp}/t_{\parallel} = 1.6$, and $t_{\perp}/t_{\parallel} = 2$. For clarity, the quasiparticle peaks were cut off at a given intensity²¹. As expected, the major feature in the antibonding channel is $4t = 2t_{\perp}$ above the bonding band. Both bands can be fitted by $(0.75 \cos k_{\parallel} - 0.47)t$ for the bonding and $(0.75 \cos k_{\parallel} - 0.47 + 4)t$ in the antibonding band (full lines in Fig. 1). However, we find additionally a clear evidence of a shadow band in the antibonding channel. This is corroborated by considering apart from the spectral function, the QP dispersion directly obtained from the imaginary time Green's function (\times with errorbars), and by superposing the fitted bonding band with an energy shift of $0.64t$, which is approximately the spin gap^{22,23}, and a momentum shift of π [dashed line in Fig. 1(b)], as expected for a shadow resulting from the coupling of the bonding band to the lowest spin excitations centered at (π, π) and with an energy given by the spin gap. The possibility of a shadow band for 2LL was first proposed on the basis of ED⁹, but due to the small system sizes, no quantitative assignment was possible. In principle, also a shadow of the antibonding band should be expected in the bonding channel. However, since the spectral weight in the antibonding channel is split between the original band and the shadow of the bonding band, resulting in rather broad features in comparison to the bonding band, less well defined shadows should be expected in this case. Only a weak structure is observed in Fig. 1(a) at around the energy of the antibonding band, but it is difficult to assign a dispersion to it.

Figure 2 presents the isotropic case $J_{\parallel} = J_{\perp} = t_{\parallel} = t_{\perp}$ for the 2LL (2×48 sites). As before, expansions around the strong coupling limit^{11,12} describe accurately the

bonding band obtained from our simulations. The high-energy excitations show no clear dispersion, and are about $5t$ higher in energy in both bands. Again, the antibonding band can be interpreted as a shadow of the bonding band. However, the energy difference between the bonding band and its shadow ($\Delta = 0.17t \pm 0.02t$) is now smaller than the value of the spin gap ($\sim J/2$)²³, which is only an upper bound that is reached when the bonding and antibonding bands are well separated as in the strong coupling case.

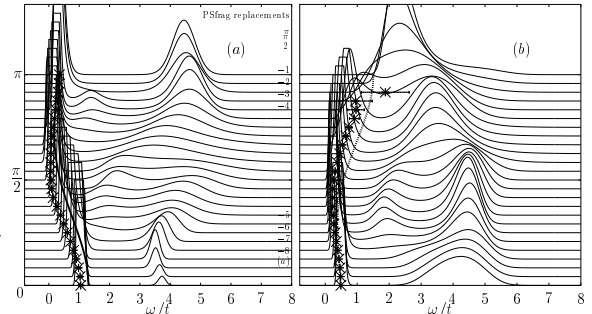


FIG. 2. Quasiparticle dispersion for the bonding (a) and antibonding (b) band for the isotropic two-leg ladder with $J/t = 1$. Further details are discussed in the text.

The lowest states for the hole in both the bonding and its shadow are now closer to $k_{\parallel} = \pi/2$ with a bandwidth $\sim 0.5t$, in rough agreement with ARPES results on $\text{Sr}_{14}\text{Cu}_{24}\text{O}_{41}$ ²⁴ in spite of the somewhat large value of J . The bands observed in ARPES are symmetric around $k_{\parallel} = \pi/2$, a feature that can be reproduced by superposing the bonding band and its shadow in Fig. 2. The very flat portions around $k_{\parallel} = \pi$ ($k_{\parallel} = 0$) for the bonding (shadow) are reminiscent of the flat dispersion around $(\pi, 0)$ or $(0, \pi)$ in two dimensions, as one approaches these points from $(0, 0)$ or (π, π) respectively, as already suggested based on a reduced basis approximation²⁵.

We consider next the 3LL and start with the strong coupling limit, where the low energy behavior was shown to correspond to an effective one-dimensional t - J -chain in the antisymmetric channel¹³, whereas ED⁵ indicate that the two symmetric channels have a finite energy gap to the antisymmetric one. The observed gap is however quite small $\sim 0.3J = 0.15t$, and therefore finite-size effects cannot be excluded. Results from DMRG^{10,26} show, that at low doping, the holes are at the two outer legs of the 3LL confirming the picture derived from ED. Figure 3 shows the spectral function for a 3LL with 3×32 sites and the same parameters as for the 2LL. As expected, the lowest state belongs to the antisymmetric channel. For $J_{\perp} \gg J_{\parallel}$, the effective parameters of the corresponding t - J chain are given by $t_{eff} = 3t_{\parallel} \left(J_{\perp} + \sqrt{J_{\perp}^2 + 8t_{\perp}^2} \right) / 8\sqrt{J_{\perp}^2 + 8t_{\perp}^2}$ and $J_{eff} = J_{\parallel}$ ¹³. Using these parameters, and a model with free spinons and holons^{27,16}, a reasonably good description of the lower edge of the antisymmetric band is obtained (full line in Fig. 3(a) corresponds to the minimal energy given

by the convolution of spinons and holons). Even more interesting are the results obtained for the two symmetric

bands. They are well separated from the antisymmetric one in energy, and can be very well fitted by the bonding

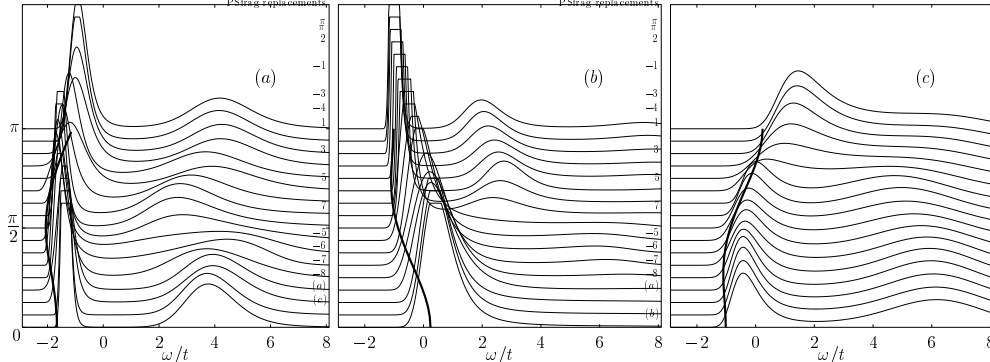


FIG. 3. Spectral function for the 3LL with $J_{\perp}/t_{\parallel} = 1.6$, $J_{\parallel}/t_{\parallel} = 0.4$, and $t_{\perp}/t_{\parallel} = 2$ in the antisymmetric (a), the symmetric bonding (b) and the antibonding (c) band. Further details are discussed in the text.

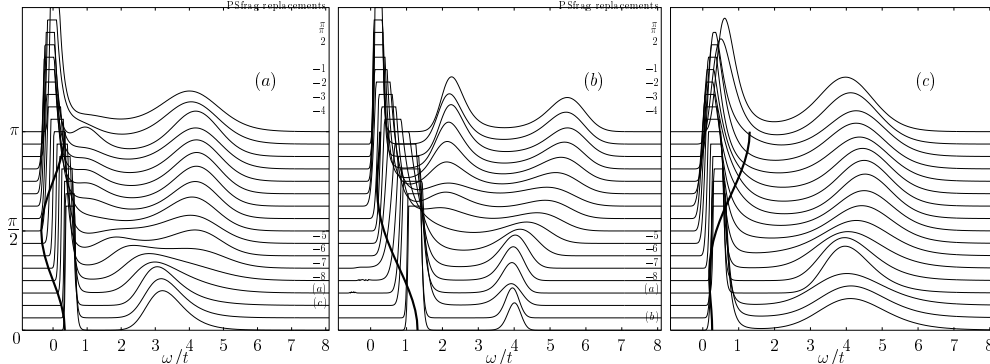


FIG. 4. Spectral function for the 3LL with $J/t = 1$. Further details are discussed in the text.

band dispersion for the isotropic 2LL from perturbation theory¹¹, with $J/t = 0.4$, and its shadow [full lines in Fig. 3(b) and (c)]. The two bands with even parity are connected by spin excitations with even parity, which are gapless^{5,28}, such that in this case no shift between them appears. The description of the 3LL system at the isotropic point ($J = t$, $t_{eff} = 0.5, 3 \times 32$ sites, Fig. 4) on the other hand, is less satisfactory when the strong coupling limit is used. All three bands have their minima around $3\pi/4$, and contrary to ED⁵, we do not find a significant energy gap between all three bands. The shape of the lower edge of the antisymmetric channel - which is determined by the holon dispersion relation for this value of $J_{eff}/t_{eff} = 2$ - differs considerably from that of the Bethe-Ansatz holon dispersion at the supersymmetric point $J/t = 2$ ²⁹.

We now address the QP weight $Z(k) = |\langle \Psi_0^{N-1}(k) | c_{\downarrow} | \Psi_0^N \rangle|^2$ which can be obtained from the imaginary time Green's function as the weight of the exponential with the slowest decay at large τt . As can be seen in Fig. 5, the QP weight is finite in the thermodynamic limit for both the bonding band and its shadow in the 2LL, and large compared to the 2D t - J

model¹⁷ (this result is valid for all k -points where the data is accurate enough to extract the QP weight). On the contrary, finite-size scaling of the QP weight in the antisymmetric channel of the 3LL leads to a vanishing QP weight in the thermodynamic limit, as expected for a Luttinger liquid. The scaling of $Z(k)$ can be fitted by $a * L^b$ with $a = 0.464 \pm 0.014, 0.564 \pm 0.015$ and $b = -0.335 \pm 0.015, -0.306 \pm 0.016$ for $J/t = 1, 2$ respectively. Squares in Fig. 5 (c) and (d) correspond to ED results that confirm the QMC ones. The values obtained for the exponent b depart from what would be obtained by naively using the strong coupling result, that for $J = t$ leads to $t_{eff} = 0.5$ (i.e. the supersymmetric case) where the exponent should be $b = -0.5$ ³⁰. In contrast to the results for the antisymmetric channel, the QP weight stays finite for the symmetric channel in the thermodynamic limit [Fig. 5(b)], although smaller than in the 2D case¹⁷. Therefore, our results demonstrate that the antisymmetric channel in the 3LL will evolve upon doping towards the Luttinger-Tomonaga universality class, whereas the symmetric channel belongs to the Luther-Emery one, as suggested previously⁵.

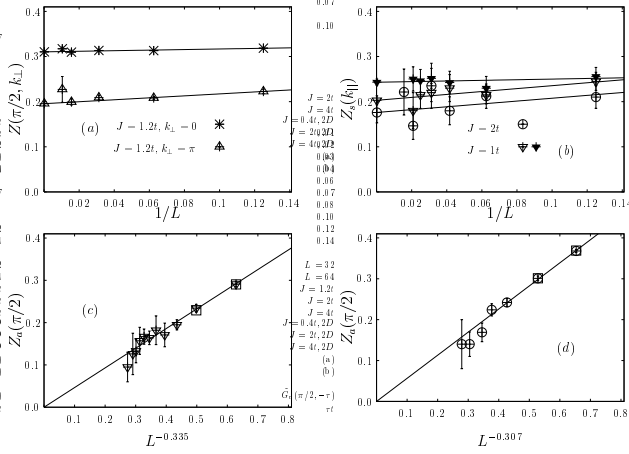


FIG. 5. Finite-size scaling for the quasiparticle weight at $k_{\parallel} = \pi/2$ for the bonding band ($k_{\perp} = 0$) and its shadow ($k_{\perp} = \pi$) in the 2LL at $J/t = 1.2$ (a), in the symmetric channel of the 3LL (b) at $J/t = 1$ and $J/t = 2$ [$k_{\parallel} = 3\pi/4$ for the bonding band (full symbols) and $k_{\parallel} = \pi/4$ for the antibonding band (open symbols)], and in the antisymmetric band of the 3LL at $k_{\parallel} = \pi/2$ for $J/t = 1$ (c), and for $J/t = 2$ (d). The squares are results from ED.

Summarizing, we have studied the spectral properties of a single hole in the t - J model on 2LL (up to 2×96 sites) and 3LL (up to 3×64 sites) using a recently developed QMC algorithm. It is shown, that expansions around the limit $J_{\perp} \gg J_{\parallel}$ describe accurately the bonding band and the high energy portion of the antibonding band in the 2LL, even in the isotropic case. However, such an expansion misses the low-energy portion of the antisymmetric channel, that corresponds to a shadow of the bonding band. For the 3LL strong coupling expansions ($J_{\perp} \gg J_{\parallel}$) for the antisymmetric channel and the 2LL give a good description of the antisymmetric and symmetric channels respectively, as long as J_{\perp} is appreciably larger than J_{\parallel} . The dispersions in the isotropic 3LL seem to be less well described by a strong coupling expansion. The QP weight extrapolates in the thermodynamic limit to a large finite value for the bonding band and its shadow in the 2LL. For the 3LL finite-size scaling leads to a vanishing QP weight for the antisymmetric channel but a finite one for the symmetric channel, demonstrating that the first one corresponds to the Luttinger universality class, whereas the latter corresponds to the Luther-Emery one.

We wish to thank D. Poilblanc, M. Troyer and O.P. Sushkov for helpful discussions. This work was supported by Sonderforschungsbereich 382 and the Australian Research Council. We thank HLRS Stuttgart and IDRIS (Orsay) for allocation of CPU time on the CrayT3E and NEC SX5, respectively.

- ¹ E. Dagotto and T. M. Rice, *Science* **271**, 618 (1996); T. M. Rice, *Z. Phys. B* **103**, 165 (1997).
- ² E. Dagotto, *Rep. Prog. Phys.* **62**, 1525 (1999).
- ³ M. Azuma, *et al.*, *Phys. Rev. Lett.* **73**, 3463 (1994); K. Kojima, *et al.*, *ibid.* **74**, 2812 (1995).
- ⁴ B. Frischmuth, S. Haas, G. Sierra, and T. M. Rice, *Phys. Rev. B* **55**, R3340 (1997).
- ⁵ T. M. Rice, S. Haas, and M. Sigrist, *Phys. Rev. B* **56**, 14655 (1997).
- ⁶ F. Zhang and T. M. Rice, *Phys. Rev. B* **37**, 3759 (1988).
- ⁷ H. Tsunetsugu, M. Troyer, and T. M. Rice, *Phys. Rev. B* **49**, 16078 (1994); R. Eder, *ibid.* **57**, 12823 (1998); J. Riera, D. Poilblanc, and E. Dagotto, *Eur. Phys. J. B* **7**, 53 (1999).
- ⁸ M. Troyer, H. Tsunetsugu, and T. M. Rice, *Phys. Rev. B* **53**, 251 (1996).
- ⁹ S. Haas and E. Dagotto, *Phys. Rev. B* **54**, R3718 (1996).
- ¹⁰ S. R. White and D. Scalapino, *Phys. Rev. B* **55**, 6504 (1997).
- ¹¹ O. P. Sushkov, *Phys. Rev. B* **60**, 3289 (1999).
- ¹² J. Oitmaa, C. J. Hamer, and Z. Weihong, *Phys. Rev. B* **60**, 16364 (1999).
- ¹³ M. Y. Kagan, S. Haas, and T. Rice, *Physica C* **318**, 185 (1999).
- ¹⁴ H. J. Schulz, *Phys. Rev. B* **59**, R2471 (1999).
- ¹⁵ J. Voit, *Eur. Phys. J. B* **5**, 505 (1998).
- ¹⁶ M. Brunner, F. F. Assaad, and A. Muramatsu, *Eur. Phys. J. B* **16**, 209 (2000).
- ¹⁷ M. Brunner, F. F. Assaad, and A. Muramatsu, *Phys. Rev. B* **62**, 15480 (2000).
- ¹⁸ H. G. Evertz, M. Marcu, and G. Lana, *Phys. Rev. Lett.* **70**, 875 (1993).
- ¹⁹ M. Jarrell and J. Gubernatis, *Phys. Rep.* **269**, 133 (1996).
- ²⁰ A. V. Chubukov, *Pis'ma Zh. Eksp. Teor. Fiz.* **49**, 108 (1989), [*JETP Lett.* **49**, 129 (1989)]; S. Sachdev and R. Bhatt, *Phys. Rev. B* **41**, 9323 (1990); S. Gopalan, T. M. Rice, and M. Sigrist, *ibid.* **49**, 8901 (1994); H. Endres, R. M. Noack, W. Hanke, D. Poilblanc, and D. Scalapino, *ibid.*, **53**, 5530 (1996).
- ²¹ This procedure was adopted in order to make smaller structures visible. The integrated value of the spectral function is normalized to $\pi/2$ for all momenta k .
- ²² T. Barnes, E. Dagotto, and E. S. Swanson, *Phys. Rev. B* **47**, 3196 (1993); T. Barnes and J. Riera, *ibid.* **50**, 6817 (1994).
- ²³ S. R. White, R. M. Noack, and D. J. Scalapino, *Phys. Rev. Lett.* **73**, 886 (1994).
- ²⁴ T. Takahashi, *et al.*, *Phys. Rev. B* **56**, 7870 (1997).
- ²⁵ G. B. Martins, C. Gazza, and E. Dagotto, *Phys. Rev. B* **59**, 13596 (1999).
- ²⁶ S. R. White and D. Scalapino, *Phys. Rev. B* **57**, 3031 (1998).
- ²⁷ H. Suzuura and N. Nagaosa, *Phys. Rev. B* **56**, 3548 (1997).
- ²⁸ B. Frischmuth, B. Ammon, and M. Troyer, *Phys. Rev. B* **54**, R3714 (1996).
- ²⁹ S. Sarkar, *J. Phys. A* **23**, L409 (1990); P.-A. Bares and G. Blatter, *Phys. Rev. Lett.* **64**, 2567 (1990); P.-A. Bares, G. Blatter, and M. Ogata, *Phys. Rev. B* **44**, 130 (1991).
- ³⁰ S. Sorella and A. Parola, *Phys. Rev. Lett.* **76**, 4604 (1996).